Shahrood University of Technology

Journal of Mining and Environment (JME)

Journal homepage: www.jme.shahroodut.ac.ir

Iranian Society of Mining Engineering (IRSME)

A Critical Review of Analytical and Semi-Analytical Approaches for Estimating the Deformation Modulus of Jointed Rock Masses

Aref Jaberi*, and Shokrollah Zare

Faculty of Mining Engineering, Petroleum and Geophysics, Shahrood University of Technology, Shahrood, Iran

Article Info

Received 14 August 2026
Received in Revised form 5 September 2026
Accepted 28 September 2026
Published online 28 September 2026

DOI: 10.22044/jme.2026.18187.3624

Keywords

Analytical Models
Semi-Analytical Models
Deformation Modulus
Jointed Rock Masses
Equivalent Continuum Models

Abstract

The deformation modulus of jointed rock masses plays a crucial role in determining the stability and deformation of rock engineering structures. Owing to its engineering significance and the complexity of discontinuity-controlled deformation, numerous approaches have been developed to estimate this parameter with varying levels of physical and computational rigor. This review critically evaluates twenty analytical and semi-analytical models published between 1968 and 2010. The models are classified into seven categories: compliance-based, orthorhombic and three-dimensional equivalent, tensorial crack or fabric, random isotropic averaging, laboratory-calibrated stiffness, non-orthogonal and dilatancy-inclusive, and hybrid nonlinear formulations, according to their mathematical structures and mechanical assumptions. The results show that joint stiffness, spacing, and orientation are the primary factors governing the deformation behavior of jointed rock masses, with shear compliance exerting the dominant influence. However, most analytical models still rely on simplified geometries, linear elasticity, and small-strain assumptions, which may limit their applicability to highly heterogeneous rock masses. Future research should focus on integrating analytical transparency with data-driven adaptability, particularly through physics-informed machine learning frameworks that combine mechanistic understanding with predictive flexibility.

1. Introduction

The deformation modulus of a rock mass is a fundamental mechanical parameter governing the response of rock engineering structures such as tunnels, caverns, slopes, foundations, and dams. It defines the ratio between applied stress and induced strain in a jointed rock mass, reflecting both elastic and inelastic deformation components. Accurate determination of this parameter is essential for reliable settlement prediction, safe support design, and long-term stability assessment. However, its evaluation remains inherently challenging because discontinuities predominantly control the deformational behavior of rock masses and introduce scale-dependent variability that cannot be captured through intact rock testing alone [1, 2]. The combination of its engineering significance and the complexity of its reliable estimation makes the deformation modulus a cornerstone parameter in rock mechanics and a continuing focus of research.

Several methodological approaches have been developed to evaluate the deformation modulus of jointed rock masses. Direct in-situ tests, including plate loading tests [3, 4], flat-jack tests—both small [5] and large [6-8], shear tests [9], pressure-chamber tests [10], radial-press tests [11], compression tests [12], dilatometer measurements [13], and borehole-jack tests [14, 15], generally yield the most representative deformation modulus values at the engineering scale. Despite their reliability, such tests are often prohibitively expensive, logistically complex, and time-consuming.

In contrast, laboratory testing of intact rock cores is simple and widely practiced in geomechanical investigations; yet these measurements consistently overestimate the

Corresponding author: Jaberi@shahroodut.ac.ir (A. Jaberi)

deformation modulus and strength, as they neglect the pervasive influence of joints, fractures, and other discontinuities that govern the mechanical behavior of rock masses. Consequently, laboratory-derived deformation modulus values cannot be directly used for design purposes without substantial correction factors [16].

Empirical approaches estimate the deformation modulus of rock masses by correlating it with commonly used rock-mass classification indices. Among various indirect evaluation techniques, these empirical correlations have received considerable attention over the past five decades. Early formulations were based on the Rock Quality Designation (RQD) index [17-22]. Subsequently, the Rock Mass Rating (RMR) system introduced by Bieniawski [16] became the foundation for a series of predictive models, which were later modified and expanded by Serafim and Pereira [23], Nicholson and Bieniawski [24], Mehrotra [25], Mitri et al. [26], Aydan et al. [27], Read et al. [28], Diederichs and Kaiser [29], Ramamurthy [30], Sonmez et al. [31], Chun et al. [32], Galera et al. [33], Isik et al. [34], Mohammadi and Rahmannejad [35], Shen et al. [36], Kang et al. [37], Khabbazi et al. [38], Kavur et al. [39], and Alemdag et al. [40]. The Q-system also provided a framework for estimating the deformation modulus [1, 41-43], while the Geological Strength Index (GSI) offered further refinements [44-48]. An alternative classification, the Rock Mass index (RMi), was later introduced by Palmström [49] for the same purpose. Beyond classification-based systems, other measurable parameters such as uniaxial compressive strength [50] and seismic wave velocity [2] have also been incorporated into empirical formulations. A summary of these empirical approaches for estimating the deformation modulus is presented in Table 1. These approaches provide a historical basis for understanding the evolution of deformation modulus estimation methods and the subsequent development of analytical and semi-analytical models.

Analytical approaches occupy an intermediate position between the simplicity of empirical correlations and the complexity of numerical simulations. Rooted in the equivalent-continuum concept, these models explicitly integrate intact rock properties with joint parameters such as normal and shear stiffness, spacing, orientation, and in-situ stress. The earliest analytical efforts focused on compliance-based formulations [51-55] and transversely isotropic or layered representations [56], which established the foundation for anisotropic analysis of the deformation modulus. These were subsequently extended into orthorhombic and fully three-dimensional constitutive laws [57-59], enabling evaluation of direction-dependent stiffness in multi-set jointed media. During the 1980s, tensorial and fabric-based models [60-63] introduced statistical representations of discontinuity geometry, while isotropic averaging formulations [64] provided simplified yet physically consistent estimates for randomly jointed rocks. Laboratory-calibrated stiffness relations [65] further bridged experimental joint mechanics with analytical prediction of the deformation modulus. Later advances incorporated nonlinear and geometric complexities, including non-orthogonal and dilatancy-coupled joint systems [66, 67], hybrid numerical–analytical models accounting for finite joint persistence [68], and unified nonlinear ubiquitous-joint frameworks describing both pre- and post-peak behavior [69]. More recent isotropic formulations [70] distilled these developments into practical closed-form relations for heavily jointed rocks. Unlike empirical methods, analytical formulations provide explicit governing equations that capture the mechanical role of discontinuities and systematically account for anisotropy, scale effects, and stress dependency, offering a physically transparent and mechanistically grounded framework for predicting the deformation modulus of rock masses.

In recent decades, numerical techniques such as the finite element method (FEM), distinct element method (DEM), and combined FEM–DEM formulations have become increasingly important for estimating the deformation modulus and compressive strength of jointed rock masses. These approaches allow explicit representation of joint geometry, heterogeneity, and anisotropy, thereby offering greater flexibility than traditional empirical methods [71-77]. However, their predictive accuracy is highly sensitive to the quality of input parameters, which must be derived from reliable laboratory or in-situ testing. Without rigorous calibration and validation, numerical predictions may remain uncertain and, in some cases, misleading.

More recently, data-driven models based on machine learning (ML) have emerged as an alternative framework for estimating the deformation modulus of rock masses. Unlike empirical correlations that rely on simplified indices or analytical and numerical methods that require explicit mechanical assumptions, ML approaches learn relationships directly from

datasets comprising intact-rock properties, joint characteristics, and in-situ measurements. Techniques such as support vector regression (SVR), Gaussian process regression (GPR), artificial neural networks (ANN), and ensemble methods (e.g., random forest, gradient boosting) have been applied with promising accuracy [78-84]. The main advantage of ML-based models lies in their ability to integrate multiple nonlinear relationships and high-dimensional parameter spaces, producing flexible and adaptive predictions. Nevertheless, their reliability strongly depends on dataset size, data quality, and the physical interpretability of the trained model. Consequently, the recent trend emphasizes hybrid ML–analytical frameworks that embed physics-informed constraints to achieve robust and practically applicable predictions of the deformation modulus.

Despite the large number of studies on the deformation modulus of rock masses, existing reviews have predominantly focused on empirical correlations or numerical simulations. In contrast, analytical methods, although grounded in strong physical principles, remain scattered across the literature and have not been synthesized in a systematic manner. To date, no comprehensive review has compiled the chronological development of analytical models, categorized them according to their mathematical formulations and mechanical assumptions, and highlighted their governing equations and applicability ranges. The novelty of this study lies in reviewing twenty analytical models published between 1968 and 2010, organizing them into a unified chronological and thematic classification, and elucidating their assumptions, strengths, limitations, and relationships to empirical indices.

Table 1. Summary of empirical approaches for estimating the deformation modulus

Classification System	Researchers	Empirical Equation
RQD and E_i	Coon and Merritt [18]	$E_m = E_i(0.0231RQD - 1.32)$
	Gardner [19]	$E_m = E_i 10^{(0.0186RQD - 1.91)}$
	Zhang and Einstein [22]	$E_m = E_i(0.0231RQD - 1.32) \quad RQD > 64\%$ $E_m = 0.15E_i \quad RQD < 64\%$
RQD, E_i and σ_c	Kayabasi et al. [20]	$E_m = 0.1423\left[\frac{E_r(1+0.01RQD)}{WD}\right]^{1.1747}$
	Gokceoglu et al. [21]	$E_m = 0.001\left[\frac{(E_r/\sigma_c)(1+0.01RQD)}{WD}\right]^{1.5528}$
RMR	Bieniawski [16]	$E_m = 2RMR_{76} - 100$
	Serafim and Pereira [23]	$E_m = 10^{(\frac{RMR_{76}-10}{40})}$
	Mehrotra [25]	$E_m = 10^{(\frac{RMR-20}{38})}$
	Aydan et al. [27]	$E_m = 9.7 \times 10^{-6} RMR^{3.54}$
	Read et al. [28]	$E_m = 0.1(RMR/10)^3$
	Diederichs and Kaiser [29]	$E_m = (7 \pm 3)\sqrt{10^{(\frac{RMR-44}{21})}}$
	Gokceoglu et al. [21]	$E_m = 0.0736\exp(0.0755RMR)$
	Chun et al. [32]	$E_m = 0.3228\exp(0.0485RMR)$
	Isik et al. [34]	$E_m = (6.7RMR - 103.06) \times 10^{-3}$
	Mohammadi and Rahmannejad [35]	$E_m = 0.0003RMR^3 - 0.0193RMR^2 + 0.3157RMR + 3.4064$
	Kang et al. [37]	$E_m = 10^{(\frac{10RMR-16}{50})}$
	Khabbazi et al. [38]	$E_m = 9 \times 10^{-7} RMR^{3.868}$
	Kavur et al. [39]	$E_m = 4^{(\frac{RMR-20}{20})}$
	Alemdag et al. [40]	$E_m = 0.058\exp(0.0785RMR)$
RMR and E_i	Nicholson and Bieniawski [24]	$E_m = 0.01E_i(0.0028RMR^2 + 0.9\exp(\frac{RMR}{22.82}))$
	Mitri et al. [26]	$E_m = 0.5E_i(1 - \cos(\frac{\pi \times RMR}{100}))$
	Ramamurthy [30]	$E_m = E_i\exp(\frac{RMR - 100}{17.4})$
	Sonmez et al. [31]	$E_m = E_i 10^{\left[\frac{(RMR-100)(100-RMR)}{4000\exp(\frac{-RMR}{100})}\right]}$
	Galera et al. [33]	$E_m = E_i\exp(\frac{RMR - 100}{36})$

Classification System	Researchers	Empirical Equation
GSI	Shen et al. [36]	$E_m = 1.14E_i\exp(-\left(\frac{RMR-116}{41}\right)^2)$
	Hoek and Brown [44]	$E_m = \sqrt{\frac{\sigma_C}{100}}10^{(\frac{GSI-10}{40})}$
	Hoek et al. [45]	$E_m = (1-\frac{D}{2})\sqrt{\frac{\sigma_c}{100}}100^{(\frac{GSI-10}{40})}$
	Gokceoglu et al. [21]	$E_m = 0.1451\exp(0.0654GSI)$
	Hoek [85]	$E_m = 0.33e^{0.064GSI}$
	Isik et al. [34]	$E_m = 5.47\times10^{-3}GSI$
	Beiki et al. [78]	$E_m = \sqrt[3]{\sigma_c}\tan(\sqrt{1.56+(\ln GSI)^2})$
	Sanei et al. [48]	$E_m = 0.0222GSI^2 - 2.1172GSI + 54.24$
GSI, E_i	Sonmez et al. [46]	$E_m = E_i(S^\alpha)^{0.4}\ ,\quad S = \exp(\frac{GSI-100}{9-3D})$
	Hoek and Diederichs [47]	$E_m = E_i\left[0.02+\frac{1-\frac{D}{2}}{1+\exp(\frac{60+15D-GSI}{11})}\right]$
Q	Barton et al. [41]	$E_m = 25\log Q$
	Barton [42]	$E_m = 10\left(Q\frac{\sigma_C}{100}\right)^{1/3}$
	Palmstrom and Singh [1]	$E_m = 8Q^{0.4}\ \ 1<Q<30$
	Kang et al. [37]	$E_m = 10^{(0.32\log Q+0.585)}$
	Ajalloeian and Mohammadi [43]	$E_m = -0.016Q^2 + 1.581Q + 0.961$
RMi	Palmstrom and Singh [1]	$E_m = 7RMi^{0.4}\quad (1<RMi<30)$
σ_c	Rowe and Armitage [50]	$E_m = 215\sqrt{\sigma_c}$
	Palmstrom and Singh [1]	$E_m = 0.2\sigma_c$
Other parameters	Ramamurthy [86]	$E_m = E_i\exp(-0.0115J_f)$
	Barton [2]	$E_m = 10\times10^{(v_p-3/5)/3}$
	Chun et al. [87]	$E_m = (5.992Depth^2 + 1.883\sigma_c^4 + 4.851RQD^3 + 0.031JS^5 + 2399.530JC)/10000$
	Beiki et al [78]	$E_m = \sqrt[3]{RQD}\log(\sigma_c).\tan(\ln(GSI))$
	Martins and Miranda [88]	$E_m = -8.1372 + 0.10005h + 0.6435UCS + 1.11458JC$
	Nejati et al. [89]	$E_m = 7.192 + 0.06469UCS + 0.20481RQD + 0.30974JSR + 0.38384JCR + 0.01716GWR$
	Kallu et al. [90]	$E_r = \exp(-0.731 + 0.08465SF + 0.382\ln(BS) + 0.134RF + 0.157IF)$

2. Methodology

The present review adopts a structured and criteria-based methodology to examine analytical approaches for estimating the deformation modulus of jointed rock masses. The scope is restricted to contributions published between 1968 and 2010, a period during which analytical modeling of the rock-mass deformation modulus experienced its most significant theoretical and practical development. Twenty representative studies were selected according to three main criteria: the study presents explicit analytical or semi-analytical formulations; the model incorporates both intact-rock and joint mechanical parameters; and the formulation has demonstrated measurable influence on subsequent analytical or engineering applications.

To enable a consistent synthesis, the selected models were classified into seven categories based on their mathematical formulation, geometrical representation, and mechanical assumptions: equivalent-continuum compliance models, orthorhombic and three-dimensional equivalent models, tensorial crack or fabric models, random-isotropic averaging models, laboratory-based joint-stiffness models, non-orthogonal and dilatancy-inclusive models, and nonlinear and hybrid analytical models.

Figure 1 illustrates the hierarchical framework adopted for this classification, highlighting the chronological evolution from early linear compliance formulations toward nonlinear and geometry-inclusive hybrid models.

This classification framework provides a coherent basis for tracing the historical evolution of analytical theories of the deformation modulus, clarifying the transition from linear compliance formulations to nonlinear and geometry-inclusive

constitutive models. Moreover, it facilitates a comparative evaluation of the selected approaches and the identification of conceptual gaps for future analytical developments.

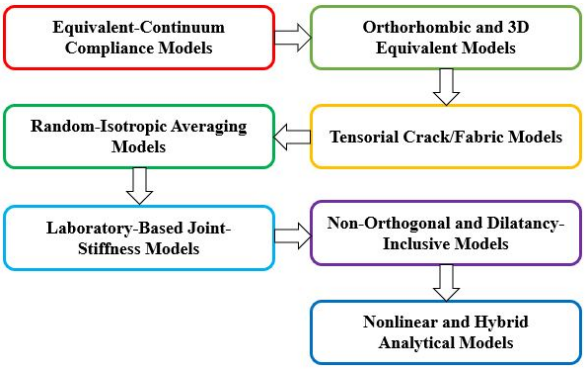

Figure 1. Conceptual evolution and thematic classification of analytical and semi-analytical models for estimating the deformation modulus of jointed rock masses.

3. Analytical models for estimating rock mass deformation modulus

3.1. Equivalent-Continuum Compliance Models

The first analytical efforts to quantify the deformation modulus of jointed rock masses were based on the equivalent-continuum concept, in which the total rock mass compliance is expressed as the sum of the compliances of the intact rock and its discontinuities. This concept was first explicitly formulated by Duncan and Goodman [51], who modeled discontinuities as zero-thickness elements characterized by normal and shear stiffnesses. Within a finite-element framework, they expressed the deformation and shear moduli of a jointed rock mass as:

$$\frac{1}{E_m} = \frac{1}{E_r} + \frac{1}{k_n S} \qquad \frac{1}{G_m} = \frac{1}{G_r} + \frac{1}{k_s S} \tag{1}$$

where E_r and G_r are the intact Young's and shear moduli, k_n and k_s are the normal and shear stiffnesses, and S is the mean joint spacing. The model assumes linear elastic behavior, zero-thickness joints, and independent deformation of each discontinuity under small-strain conditions. Although simplified, it established the foundation for the analytical treatment of jointed rock deformability and later inspired compliance-matrix approaches. Singh [52] developed a general compliance-matrix formulation for jointed rock masses, explicitly incorporating joint stiffness, spacing, and orientation. The total compliance matrix was written as:

$$[M] = [M_r] + n\left[K_j\right]^{-1}\left[B_j\right] \tag{2}$$

where $[M]$ and $[M_r]$ are the compliance matrices of the jointed and intact media, n is the joint frequency, and $\left[K_j\right]$ and $\left[B_j\right]$ denote the stiffness and orientation matrices of each joint set. Simplified scalar expressions for the directional moduli were obtained as:

$$\frac{1}{E_m} = \frac{1}{E_r} + \frac{n}{k_n} \qquad \frac{1}{G_m} = \frac{1}{G_r} + \frac{n}{k_s} \tag{3}$$

These relations demonstrate that the deformation modulus E_m and shear modulus G_m decrease with increasing joint frequency and decreasing joint stiffness. Singh [53] emphasized that the reduction in shear modulus is generally greater than that in deformation modulus, explaining the significant lateral deformation observed in jointed rock masses. The formulation assumes linear elasticity, small-strain behavior, and independent deformation of joint sets, and is most reliable for moderately jointed rocks under low stress gradients. This model represents a fundamental analytical framework for describing anisotropic deformation modulus, later forming the basis for orthorhombic and 3-D equivalent models. Kulhawy [54] refined the equivalent-compliance approach by deriving explicit analytical expressions for both deformation and shear moduli of rock masses containing three orthogonal joint sets. The relations were expressed as:

$$\frac{1}{E_i} = \frac{1}{E_r} + \frac{1}{k_{i,n} S_i} \qquad \frac{1}{G_{ij}} = \frac{1}{G_r} + \frac{1}{k_{j,s} S_j} \tag{4}$$

where S_j is the mean spacing of the *i*-th joint set, and $k_{i,n}$ and $k_{j,s}$ are the normal and shear stiffnesses. Kulhawy [54] further introduced a semi-empirical correlation between the analytical modulus and the Rock-Quality Designation (RQD), approximately expressed as:

$$\frac{E_m}{E_r} = 0.1 + 0.9\frac{RQD}{100} \tag{5}$$

This correlation, derived from field-data trends, provided a practical means of estimating rock-mass deformation modulus directly from RQD values. The model assumes orthogonal, regularly spaced,

zero-thickness joints with linear elastic behavior, and is therefore most reliable for moderately jointed, small-strain rock masses. While the approach successfully linked analytical compliance theory with empirical field characterization, it remains limited for irregular or intersecting joint systems where the assumption of perfect orthogonality is not valid. Dershowitz et al. [55] introduced a probabilistic extension of the compliance formulation, representing joint geometry statistically through a joint spacing–orientation probability density function $P(s,\theta)$. The expected average compliance of the rock mass was expressed as:

$$\langle J_m \rangle = \int P(S,\theta)\Delta J(S,\theta) dS d\theta + J_r \quad (6)$$

from which the expected deformation and shear moduli follow:

$$\langle E_m \rangle, \langle G_m \rangle = \int P(S,\theta)[E(S,\theta), G(S,\theta)] dS\, d\theta \quad (7)$$

where J_m and J_r denote the macroscopic and intact rock compliances, $\Delta J(S,\theta)$ is the incremental compliance of discontinuities with spacing S and orientation θ, $P(S,\theta)$ is the joint spacing–orientation probability density, and $E(S,\theta)$, $G(S,\theta)$ are the local deformation and shear moduli of each joint set. This probabilistic framework incorporates the stochastic variability of joint spacing and orientation, allowing the computation of mean macroscopic moduli from random joint configurations. The model assumes linear elastic joints, independent displacements at intersections, and homogeneous stress fields, making it applicable primarily to hard rocks under small-strain conditions. It provides a rational explanation for the wide scatter observed in field-measured deformation moduli by demonstrating that random variations in joint geometry alone can produce substantial dispersion in equivalent moduli.

Collectively, the compliance-matrix frameworks of Duncan and Goodman [51] and Singh [52,53], the analytical–empirical relations of Kulhawy [54], and the stochastic formulation of Dershowitz et al. [55] established a fundamental theoretical framework for deformation-modulus estimation in jointed rocks. These models demonstrated that rock-mass deformation is primarily controlled by discontinuity characteristics, particularly joint stiffness, spacing, frequency, and orientation, with shear compliance often exerting a dominant influence on the overall mechanical response. Despite the simplifications associated with representing discontinuous rock masses as equivalent continua, these formulations provide a mechanically based framework derived from continuum mechanics and elastic homogenization concepts, where discontinuity properties are incorporated into equivalent compliance or elastic parameters rather than empirical correction factors. However, their applicability depends on assumptions such as representative averaging of discontinuity characteristics, linear elastic behavior, and small-strain conditions. Consequently, their predictive capability may be limited in highly heterogeneous rock masses where irregular fracture networks, strong joint interactions, or nonlinear deformation mechanisms dominate.

3.2. Orthorhombic and 3D Equivalent Models

Analytical formulations of rock-mass deformation modulus evolved beyond simple compliance relations toward fully three-dimensional orthorhombic representations that explicitly incorporated multiple joint sets, direction-dependent stiffness, and anisotropy. These developments marked the transition from scalar modulus correlations to tensorial constitutive descriptions.

Salamon [56] presented one of the earliest analytical treatments of layered rock masses, modeling them as transversely isotropic equivalent continua using the principle of strain-energy equivalence. A layered medium was represented by an equivalent continuum with five independent elastic constants, whose effective parameters were obtained as thickness-weighted harmonic averages of the layer moduli:

$$E_1 = \left(\sum \frac{\varphi_i}{E_{1i}}\right)^{-1} \quad E_2 = \left(\sum \frac{\varphi_i}{E_{2i}}\right)^{-1} \quad G_2 = \left(\sum \frac{\varphi_i}{G_{2i}}\right)^{-1} \quad (8)$$

where φ_i is the thickness fraction of the i-th layer, and E_{1i}, E_{2i}, G_{2i} are the moduli of each constituent layer. This framework presumes perfect interlayer bonding, linear elasticity, and small strains, while interlayer slip and separation are neglected. Although originally developed for stratified rocks, Salamon's formulation established the conceptual basis for representing discontinuous or layered systems as equivalent anisotropic continua with directional elastic properties. Amadei and Goodman [57] introduced one of the first fully three-dimensional constitutive relations

for jointed rock masses, where the total strain was expressed as the sum of the intact rock compliance and the contribution of each joint set:

$$\varepsilon_{ij} = \sum_{n} D_{ijkl}^{rock}\sigma_{kl} + D_{ijkl}^{joint,n}\sigma_{kl} \quad (9)$$

where D_{ijkl}^{rock} and $D_{ijkl}^{joint,n}$ denote the compliance tensors of the intact rock and the n-th joint set, respectively. For orthogonal joint sets, the direction-dependent deformation and shear moduli were derived as:

$$E_x = \left(\frac{1}{E_r} + \frac{1}{k_{nx}S_x}\right)^{-1}$$
$$G_{xy} = \left(\frac{1}{G_r} + \frac{1}{k_{sx}S_x}\right)^{-1} \quad (10)$$

where E_r, G_r are the intact Young's and shear moduli, k_n, k_s represent the normal and shear stiffnesses of joints, and S is the mean spacing. This model presumes linear joint behavior, orthogonal and persistent joint sets, and small strains, while joint interaction and slip are neglected. It provided the first comprehensive 3D analytical framework combining intact rock and joint properties within a unified compliance-based approach, clearly showing how directional stiffness reduction governs the anisotropic deformation modulus of jointed rocks.

Gerrard [58] extended the orthorhombic equivalent-continuum theory to rock masses containing one, two, or three orthogonal joint sets, representing them as equivalent homogeneous orthorhombic continua. The governing relations retained the same compliance-based form as earlier formulations but emphasized the anisotropic stiffness reduction caused by shear deformation:

$$E_y = \left(\frac{1}{E_r} + \frac{1}{k_{ny}S_y}\right)^{-1}$$
$$G_{yz} = \left(\frac{1}{G_r} + \frac{1}{k_{sy}S_y}\right)^{-1} \quad (11)$$

where E_r, G_r denote the intact Young's and shear moduli, k_n, k_s are the joint normal and shear stiffnesses, and S represents the mean joint spacing. The framework assumes very thin, linearly elastic, and non-dilatant joints under small strains and applies primarily to regularly jointed rocks with orthogonal geometry. Gerrard demonstrated that shear moduli experience a greater reduction than normal moduli, a finding consistent with both laboratory and field observations, and highlighted the engineering relevance of orthorhombic anisotropy in controlling the deformation and stability of jointed rock masses.

Amadei and Savage [59] generalized the orthorhombic equivalent-continuum model to account for non-orthogonal joint systems and directional loading. The deformation modulus was expressed as an orientation-dependent function:

$$E_m(\theta) = \left[\sum_{i} \frac{1}{E_r} + \frac{f(\theta_i)}{k_{ni}S_i}\right]^{-1} \quad (12)$$

where $f(\theta_i)$ is an orientation factor that describes the angle between the joint normal and the loading direction. This formulation presumes linear joint stiffness, small strain, and no joint-intersection interaction, making it applicable primarily to regular joint networks with uniform stress fields. The model linked stiffness anisotropy with strength reduction, providing one of the earliest unified analytical frameworks to describe both deformation modulus and failure in jointed rock masses.

From Salamon's [56] transversely isotropic continuum model to the three-dimensional formulations of Amadei and Goodman [57], Gerrard [58], and Amadei and Savage [59], this second generation of analytical models established a fundamental framework for anisotropic deformation-modulus analysis in rock mechanics. Together, they bridged the gap between planar compliance theories and modern tensorial or numerical formulations, forming a fundamental analytical basis for describing directional stiffness in jointed rock masses. Despite their capability in representing directional deformation behavior, orthorhombic and three-dimensional equivalent models still rely on homogenization concepts to transform complex jointed structures into directional continuum properties. Their main advancement over scalar compliance models lies in the representation of anisotropy through stiffness and compliance tensors, allowing the effects of joint orientation and spatial arrangement to be explicitly incorporated. These models are most appropriate when dominant joint sets can be identified and their directional characteristics can be reasonably quantified. However, their applicability may decrease in highly fractured rock masses with complex joint geometries, strong interaction between discontinuities, or localized nonlinear deformation, where directional homogenization may not adequately capture the governing deformation mechanisms.

3.3. Tensorial Crack and Fabric Models

Oda advanced the analytical modeling of jointed and cracked rock masses by introducing the fabric/crack tensor concept, which enabled the statistical geometry of discontinuities—orientation, density, and size—to be incorporated directly into constitutive relations. This approach overcame the limitations of orthogonal joint set assumptions and established a unified tensorial framework for representing anisotropy in jointed rocks.

In his seminal study, *Fabric Tensor for Discontinuous Geological Materials*, Oda [60] defined a second-order fabric tensor as a statistical descriptor of the orientation and frequency of discontinuities within a representative volume:

$$F_{ij} = \int n_i n_j E(n) d\Omega \tag{13}$$

where n_i and n_j are the direction cosines of the discontinuity normal, $E(n)$ is the orientation density function, and $d\Omega$ is the differential solid-angle element for orientation integration. This tensor quantitatively captures the directional bias within the discontinuity system and provides a rigorous geometrical basis for describing anisotropy in rock masses. The 1982 formulation [60] was geometrical in nature and did not yet provide explicit mechanical expressions for the deformation or shear modulus. It assumes a statistically homogeneous discontinuity distribution, linear elasticity, and a representative elementary volume large enough to capture the statistical orientation of cracks.

Since this formulation only describes the geometric fabric of discontinuities, it does not account for mechanical interaction or scale-dependent effects, and its applicability decreases for highly clustered discontinuity systems. Building upon this geometrical foundation, Oda [61] developed the first tensorial compliance formulation for cracked rock materials, extending the 1982 concept into a mechanical framework. The general constitutive relation was expressed as:

$$\varepsilon_{ij} = \alpha F_{ijkl} \sigma_{kl} + D^0_{ijkl} \sigma_{kl} \tag{14}$$

where D^0_{ijkl} is the compliance tensor of the intact rock, F_{ijkl} is a fourth-order crack tensor derived statistically from F_{ij}, and α is a material constant representing crack compliance intensity.

This formulation provided the mechanical linkage between crack geometry and elastic compliance, forming the theoretical foundation of the equivalent-continuum representation for randomly cracked rock masses. Similar to the 1982 framework, it did not yield explicit scalar expressions for the deformation or shear modulus; instead, anisotropy was described through tensor components. The framework presumes linear elasticity, low crack density, and negligible crack–crack interaction within a statistically homogeneous medium. It tends to overestimate stiffness at high crack densities because elastic interactions and stress-dependent crack closure are neglected. Extending this mechanical concept, Oda [62] formulated a hydro-mechanically coupled equivalent-continuum model that incorporated both mechanical deformation and fracture-controlled permeability. The total strain tensor was written as the sum of the intact-matrix and joint-induced compliances:

$$\varepsilon_{ij} = M_{ijkl} \sigma_{kl} + (p\delta_{kl} - C_{ijkl} \sigma_{kl}) \tag{15}$$

where M_{ijkl} and C_{ijkl} denote the compliance tensors of the intact matrix and the joint system, respectively, p is the pore pressure, and δ_{kl} is the Kronecker delta. For joint systems characterized by normal and shear stiffnesses k_n and k_s, and mean spacing S, the equivalent moduli were expressed explicitly as:

$$\frac{1}{E_m} = \frac{1}{E} + \frac{1}{k_n S}$$
$$G_m = \frac{1}{G} + \frac{1}{k_s S} \tag{16}$$

This work further extended Oda's framework by providing explicit analytical expressions for the deformation and shear moduli of a jointed rock mass. The model presumes linear elastic and independent joint behavior, small strains, and an impermeable rock matrix through which fluid flow occurs only via fractures. It neglects crack interactions and stress-dependent closure and is valid mainly for low crack densities and elastic deformation ranges. This work established an analytical tensorial framework coupling stress–deformation and fluid flow, thereby unifying mechanical and hydraulic anisotropy in rock masses.

Through laboratory experiments on mylonite specimens containing randomly oriented cracks, Oda [63] validated the theoretical predictions of his tensorial framework and proposed simplified empirical relations for modulus reduction:

$$\frac{E'}{E} = \frac{1}{1+\alpha F_{11}}$$
$$\frac{G'}{G} = \frac{1}{1+\beta F_{ij}} \quad (17)$$

where F_{11} and F_{ij} are principal components of the fabric tensor, α, β are empirically determined constants, E' and G' are effective Young's and shear moduli, with E and G representing the corresponding intact moduli.

This experimental study marked the first explicit empirical formulation linking crack density and orientation to both deformation and shear modulus, confirming that shear modulus reduction is generally more pronounced than normal stiffness degradation. The framework presumes linear elasticity and isotropic matrix behavior with randomly oriented, non-interacting cracks and purely recoverable deformations. However, it neglects crack interaction and permanent slip and remains valid only within the elastic range for low crack densities.

Building upon his earlier theoretical and numerical studies [60–62], the 1988 work [63] validated the complete tensorial–mechanical framework and demonstrated the quantitative correlation between crack density, orientation anisotropy, and modulus reduction. Collectively, the four studies by Oda [60–63] represent a progressive evolution from purely geometrical to analytically and experimentally validated formulations. The 1982 and 1984 works [60, 61] established the statistical and tensorial foundations, while the 1986 and 1988 studies [62, 63] introduced explicit analytical and empirical expressions for the deformation and shear moduli. Together, they constitute a comprehensive tensorial framework bridging microstructural crack statistics and macroscopic equivalent-continuum deformation in jointed rock masses. Despite their strong micromechanical basis, tensorial crack and fabric models rely on statistical characterization of discontinuity networks and require a representative volume element containing sufficient crack information for reliable application. Their mechanical validity originates from continuum mechanics and tensorial constitutive formulations, where crack geometry, density, size, and orientation are directly linked to equivalent compliance and elastic properties. However, their applicability is mainly limited to fractured rock masses where discontinuity distributions can be statistically represented and deformation remains within an elastic or quasi-elastic regime. The predictive capability of these models may decrease when deformation is governed by significant crack–crack interactions, progressive crack growth, permanent slip, or highly localized nonlinear mechanisms that cannot be fully captured through statistical tensorial representations.

3.4. Random-isotropic averaging model

Fossum [64] introduced a closed-form isotropic model based on statistical averaging of joint orientations within a composite-material framework. Unlike the anisotropic tensorial and orthorhombic frameworks of the previous decade, Fossum's approach assumed that when discontinuities are randomly distributed in space, the overall mechanical response of the rock mass can be treated as isotropic.

The intact rock is characterized by its Young's modulus E_r and Poisson's ratio υ_r, while discontinuities are represented by their normal and shear stiffnesses k_n and k_s. By integrating the stiffness contributions of joints over all possible orientations, Fossum derived analytical expressions for the effective bulk K_m and shear G_m moduli of the equivalent isotropic continuum:

$$K_m = \frac{E_r}{9}\left[\frac{3(1+\upsilon_r)sk_n + 2E_r}{(1+\upsilon_r)(1-2\upsilon_r)sk_n + (1-\upsilon_r)E_r}\right]$$
$$G_m = \frac{1}{30}\left[\frac{E_r}{(1+\upsilon_r)}\frac{9(1+\upsilon_r)(1-2\upsilon_r)sk_n + (7-5\upsilon_r)E_r}{(1+\upsilon_r)(1-2\upsilon_r)sk_n + (1-\upsilon_r)E_r}\right] + \frac{2}{5}\left[\frac{E_r sk_s}{2(1+\upsilon_r)sk_s + E_r}\right] \quad (18)$$

From these expressions, the equivalent Young's modulus and Poisson's ratio of the jointed rock mass are obtained as:

$$E_m = \frac{9K_mG_m}{3K_m + G_m}$$
$$\upsilon_m = \frac{3K_m - 2G_m}{2(3K_m + G_m)} \quad (19)$$

These relations show that as the mean joint spacing S increases or as joint stiffnesses k_n and k_s

become large, the effective moduli E_m and G_m approach the intact values. Conversely, for highly fractured or compliant rock masses, both moduli decrease rapidly, reflecting the dominant influence of joint deformation on bulk mechanical response. This framework assumes linear elastic behavior, randomly distributed joints, negligible joint interactions, and joint thickness much smaller than the mean spacing. It remains valid for small strains and statistically isotropic discontinuity distributions. However, the formulation is restricted to low crack densities and random joint orientations, neglecting nonlinear joint closure and slip. Consequently, it cannot accurately capture anisotropic behavior in regularly jointed or directionally persistent rock masses.

Fossum [64] demonstrated that this isotropic formulation is theoretically consistent with the results of more complex anisotropic theories [57, 61], while offering a far simpler analytical means of estimating the rock mass deformation modulus. The closed-form nature of the model makes it practical for design and numerical analyses requiring only measurable parameters. By transforming anisotropic mechanical properties into statistically averaged isotropic behavior, Fossum [64] demonstrated that the average mechanical response of randomly jointed rock masses can be effectively captured through isotropization without sacrificing physical realism. His model, therefore, represents a comprehensive analytical approach for isotropizing jointed rock-mass deformation while preserving the essential mechanics associated with joint stiffness and spacing. Although Fossum's isotropic averaging model provides a mechanically based framework derived from elastic constitutive theory and composite-material averaging concepts, its validity primarily depends on the assumption that discontinuity orientations are randomly distributed at the representative scale. By averaging the directional effects of joints, the model provides a simplified estimation of bulk elastic properties while retaining the contribution of joint stiffness and spacing. However, this isotropic approximation may not be appropriate for rock masses containing persistent joint sets or strong directional structures, where deformation is governed by anisotropic behavior. Therefore, its predictive capability decreases when directional discontinuity patterns or stress-dependent joint behavior dominate the mechanical response.

3.5. Joint stiffness driven laboratory model

Analytical models of the mid-1980s began integrating laboratory-derived joint-stiffness parameters, bridging theoretical compliance formulations with experimentally observed rock joint behavior [65]. Yoshinaka and Yamabe [65] developed a constitutive relation for evaluating the deformation behavior of discontinuous rocks, directly linking the normal and shear stiffnesses of joints to the equivalent deformation and shear moduli of jointed rock masses. Their work emphasized the mechanical response of rock-joint systems under varying confining pressures and joint orientations, incorporating the effects of surface roughness, stress level, and interlocking mechanisms. The formulation presumes that the overall deformation of a rock mass can be represented by a summation of the deformation contributions from intact rock and joints. For a rock mass containing two joint sets inclined at angles θ_1 and θ_2 to the loading direction, the tangent (directional) Young's modulus E_t and shear modulus G_t were expressed as:

$$E_t = \left[\frac{1}{E_r} + \frac{\cos^2\theta_1}{L_1}\left(\frac{\sin^2\theta_1}{k_{s1}} + \frac{\cos^2\theta_1}{k_{n1}}\right) + \frac{\cos^2\theta_2}{L_2}\left(\frac{\sin^2\theta_2}{k_{s2}} + \frac{\cos^2\theta_2}{k_{n2}}\right)\right]^{-1}$$

$$G_t = \left[\begin{array}{l} \dfrac{2(1+\upsilon_r)}{E_r} + \dfrac{\cos^2\theta_1}{L_1}\left(\dfrac{2\sin^2\theta_1 + |\sin\theta_1|2}{k_{s1}} + \dfrac{2\cos^2\theta_1 - |\sin2\theta_1|/2}{k_{n1}}\right) \\ \quad \dfrac{\cos^2\theta_2}{L_2}\left(\dfrac{2\sin^2\theta_2 + |\sin2\theta_2|2}{k_{s2}} + \dfrac{2\cos^2\theta_2 - |\sin2\theta_2|/2}{k_{n2}}\right) \end{array}\right]^{-1} \quad (20)$$

where E_r and υ_r denote the Young's modulus and Poisson's ratio of the intact rock, L_i is the mean spacing of the i-th joint set, θ_i is the dip angle of the joint plane relative to the loading axis, k_{ni} and k_{si} are the corresponding normal and shear stiffnesses of each joint set. These relations clearly demonstrate that both the normal and shear deformation of a jointed rock mass depend on the geometric and mechanical properties of its discontinuities. As joint spacing increases or stiffness becomes large, the effective moduli E_t and G_t approach those of the intact rock. Conversely,

for highly jointed or soft discontinuity systems, both moduli decrease rapidly, capturing the strong compliance introduced by joint deformation. The analytical formulation presumes linear elasticity, zero-thickness joints, and plane-stress conditions involving two orthogonal joint sets. Joint sets are considered independent and non-dilating, and coupling effects between shear and normal deformations are neglected. The model remains valid for small-strain, pre-yield conditions and does not account for nonlinear closure or joint slip.

Yoshinaka and Yamabe [65] validated their model through laboratory compression and shear tests on welded tuff and granite blocks containing one or two joint sets under confining pressures up to 2 MPa. The experimental results confirmed that the model accurately predicts the directional variation of stiffness, the nonlinear closure of joints under increasing normal stress, and the pronounced reduction of shear modulus relative to the deformation modulus. This study bridged micro-scale joint mechanics with macro-scale rock-mass deformation, offering one of the earliest physics-based analytical models capable of predicting anisotropic, stress-dependent stiffness in jointed rock masses. The mechanical basis of Yoshinaka and Yamabe's formulation lies in the incorporation of joint stiffness parameters into an equivalent-continuum framework, where the contribution of discontinuities to rock mass deformation is explicitly considered. By relating normal and shear joint stiffnesses to equivalent deformation properties, the model provides a physically based interpretation of modulus reduction rather than relying solely on empirical correlations. However, its applicability depends on the accurate characterization of joint properties and is mainly suitable for regularly jointed rock masses. Its predictive capability may decrease when deformation is governed by complex joint interactions, progressive damage, or strongly nonlinear discontinuity behavior.

3.6. Nonorthogonal and dilatancy-inclusive Models

Analytical progress in evaluating the deformation modulus of jointed rock masses has incorporated the effects of nonlinear joint behavior, non-orthogonal intersection geometry, and joint dilatancy, representing a significant advance beyond earlier linear orthorhombic formulations. Two influential contributions in this category were presented by Chen [66] and Huang et al. [67], which collectively expanded analytical modeling to capture the complex mechanical response of discontinuous rock systems.

Chen [66] proposed a nonlinear constitutive model for rock masses containing two orthogonal joint sets, where the rock mass was treated as a continuous elastic matrix intersected by planar discontinuities obeying nonlinear stress–strain laws. Unlike earlier linear elastic approaches, Chen's formulation reproduced both elastic and post-peak strain-softening behavior. The total strain tensor was defined as the sum of intact-rock and joint-induced strains.

$$\varepsilon_{ij} = \sum_{k} \varepsilon_{ij}^{m} + \varepsilon_{ij}^{(k)} \tag{21}$$

where ε_{ij}^{m} is the strain of the intact matrix and $\varepsilon_{ij}^{(k)}$ is the contribution from the *k*-th joint set. Although Chen's model did not yield explicit analytical equations for the deformation or shear modulus, it provided closed-form stress–strain relationships that captured nonlinear joint closure and post-peak shear softening. By doing so, it extended analytical treatments of the deformation modulus to include both nonlinearity and dilatancy effects. This model was among the first to incorporate nonlinear pre- and post-peak joint behavior within a continuous analytical framework, forming the basis for later ubiquitous-joint models implemented in numerical codes such as FLAC and UDEC.

Building on this foundation, Huang et al. [67] further developed the analytical formulation of jointed rock deformability by deriving closed-form expressions for the elastic moduli of rock masses containing three non-orthogonal joint sets. Their model explicitly incorporated the intersection angle θ, mean spacing s, and joint stiffness components (k_n, k_s), providing direction-dependent formulations for the deformation and shear moduli:

$$\frac{1}{E_y} = 2\sin^2(\frac{\theta}{2})\frac{\cos^2(\frac{\theta}{2})k_n + \sin^2(\frac{\theta}{2})k_s}{k_n k_s s} \qquad \frac{1}{E_z} = 2\cos^2(\frac{\theta}{2})\frac{\sin^2(\frac{\theta}{2})k_n + \cos^2(\frac{\theta}{2})k_s}{k_n k_s s}$$

$$\frac{1}{G_{xy}} = \frac{1}{k_{s3}s_3} + \frac{2\sin\theta\cos^2(\frac{\theta}{2})}{k_s s} \qquad \frac{1}{G_{yz}} = \frac{2\sin^2\theta(k_n + k_s)}{k_n k_s s} \qquad \frac{1}{G_{zx}} = \frac{1}{k_{s3}s_3} + \frac{2\sin\theta\sin^2(\frac{\theta}{2})}{k_s s} \tag{22}$$

where E_y, E_z are the directional Young's moduli, G_{xy}, G_{yz}, G are the corresponding shear moduli. The model demonstrated that as θ deviates from 90°, anisotropy in deformation modulus increases sharply, while shear moduli exhibit stronger reductions than deformation moduli, consistent with experimental findings. The formulation assumed three non-orthogonal joint sets under small-strain linear behavior, uniform stress distribution, and no joint-intersection interactions. Because the stress field was assumed homogeneous and joint interlocking effects were neglected, the model tended to provide lower-bound estimates of the elastic moduli. Experimental validation on plaster block models confirmed that the analytical predictions closely matched measured values, particularly when joint dilatancy was included, highlighting the importance of shear-induced volumetric coupling.

In summary, Chen [66] introduced a nonlinear constitutive framework capturing both pre- and post-peak joint behavior, while Huang et al. [67] extended it to a geometrically explicit model that accounted for non-orthogonal intersections and dilatancy effects. Together, these studies mark a pivotal step toward realistic constitutive modeling of jointed rock masses, encompassing nonlinear stress–strain behavior and geometric anisotropy within analytical formulations. The formulations developed by Chen [66] and Huang et al. [67] provide a mechanically based extension of equivalent-continuum models by incorporating joint orientation, spacing, and stiffness into constitutive descriptions of fractured rock masses. Their theoretical basis extends continuum homogenization by incorporating orientation-dependent and nonlinear responses of discontinuities, where discontinuity-induced deformation is represented through additional flexibility components rather than empirical correction factors. These models are mainly applicable to regularly fractured rock masses that can be represented by equivalent elastic parameters under small-strain conditions. However, their applicability is limited by assumptions regarding representative joint characterization, simplified joint interactions, and stress conditions. Therefore, their predictive capability may decrease in highly heterogeneous rock masses where complex fracture networks, extensive joint interactions, and deformation mechanisms beyond the assumed constitutive framework dominate.

3.7. Advanced Hybrid and Nonlinear Models

Analytical modeling of rock mass deformation modulus has evolved toward hybrid, geometry-informed, and nonlinear constitutive frameworks capable of representing realistic fracture network geometry and capturing both pre- and post-peak deformation behavior. This new generation of models emphasizes numerical calibration, nonlinear stress–strain relationships, and integration with numerical solvers, marking the transition from purely analytical formulations to semi-analytical and field-calibrated approaches.

Kulatilake et al. [68] pioneered one of the first three-dimensional hybrid methods combining numerical distinct-element modeling (3DEC) with analytical fracture-tensor formulations. In their study, rock blocks containing finite-sized, non-persistent joints were simulated, and the influence of geometric parameters such as joint orientation, density, size, and persistence on the deformation modulus was systematically evaluated. They introduced a stochastic joint network generator coupled with 3DEC to compute direction-dependent moduli, demonstrating that assuming infinite joint persistence leads to an underestimation of stiffness. Conversely, incorporating finite joint lengths yields higher equivalent moduli due to partial load transfer through intact rock bridges. From these numerical observations, semi-analytical power-law relations were proposed to link equivalent deformation moduli with fracture-tensor components:

$$B\left(F_{ij}\right)^{\beta} = A_{ij}(F_{ii})^{\alpha} \quad G = E_i \tag{23}$$

Where F_{ij} are the fracture tensor components representing joint orientation and density, and A, B, α , and β are empirically fitted constants. The formulation assumes a linear elastic intact rock, small strains, and no joint dilatancy. Because these constants depend on stress level and joint configuration, the model must be calibrated for each rock mass type. This hybrid tensor–DEM framework effectively captured anisotropy and scale dependence of rock mass stiffness and was later implemented as an incrementally linear orthotropic constitutive law.

Wang and Huang [69] advanced this concept by developing a nonlinear semi-analytical constitutive model for rock masses containing multiple ubiquitous joint sets. Their model integrated both pre-peak elastic and post-peak strain-softening behavior, defining the total strain as the sum of intact rock and joint-induced components:

$$d\varepsilon = \sum_{a} d\varepsilon_a^J + d\varepsilon^I \quad (24)$$

where $d\varepsilon^I$ and $d\varepsilon_a^J$ denote the strain increments of the intact rock matrix and the a-th joint set, respectively. Each joint set was described by a compliance matrix with evolving normal and shear components:

$$k_n = \frac{1}{D_{nn}} \qquad k_s = \frac{1}{D_{ss}} \quad (25)$$

where D_{nn} represents the normal compliance associated with nonlinear joint closure, while k_n and k_s evolve according to Barton's JRC–JCS shear law, representing roughness degradation and post-peak softening. Although formulated analytically, the model is semi-analytical because equivalent stiffness is obtained implicitly as a tangent modulus from nonlinear stress–strain curves rather than from closed-form equations. It delineates the complete deformation process into four distinct stages: closure, pre-peak, peak, and post-peak, while incorporating joint closure, shear dilatancy, and roughness degradation through evolving compliance terms. The model assumes small strains, ubiquitous joint sets, and no direct joint–joint interaction. It was implemented in FLAC as a user-defined constitutive law, bridging analytical formulations with numerical simulation in rock-mass deformation analysis.

Zhang [70] introduced a closed-form isotropic analytical model for heavily jointed rock masses based on equivalent-continuum averaging. Using composite compliance between intact rock and randomly oriented discontinuities, the equivalent deformation and shear moduli were expressed as:

$$E_m = \frac{1}{\frac{1}{E_r} + \frac{1}{3}\left[\frac{21}{32k_nS} + \frac{11}{32k_sS}\right]} \qquad G_m = \frac{1}{\frac{1}{G_r} + \frac{1}{3}\left[\frac{11}{32k_nS} + \frac{21}{32k_sS}\right]} \quad (26)$$

where E_r, G_r are the intact Young's and shear moduli, k_n and k_s are joint normal and shear stiffnesses, and S is the mean joint spacing. The model assumes a linear elastic, isotropic intact rock and randomly distributed thin joints. By statistically averaging stiffness contributions, Zhang's formulation [70] provided a practical means to estimate the deformation modulus of heavily jointed rocks. Results consistent with laboratory and field data confirmed that the model effectively predicts average modulus reduction due to random jointing. However, the assumptions of isotropy and linear elasticity limit its applicability to directional or sparsely jointed rock masses.

The evolution from Kulatilake et al. [68] through Wang and Huang [69] to Zhang [70] reflects the progressive development of deformation-modulus models from geometry-based hybrid approaches toward nonlinear constitutive and simplified engineering formulations. Kulatilake et al. [68] introduced hybrid tensor–DEM concepts incorporating finite joint geometry and scale effects, whereas Wang and Huang [69] advanced analytical models toward nonlinear, stress-dependent constitutive descriptions. Zhang [70] further simplified equivalent-continuum formulations for practical estimation of deformation modulus in heavily jointed rocks. These hybrid and nonlinear approaches provide a more realistic representation of fractured rock masses by incorporating finite fracture geometry, stress-dependent joint behavior, and numerical calibration within equivalent-continuum frameworks. However, their increased realism is accompanied by higher requirements for input characterization and calibration, which may restrict their application when detailed fracture information is unavailable. Overall, these developments represent a transition from earlier linear compliance-based formulations toward geometry-inclusive, nonlinear, and hybrid analytical–numerical frameworks that continue to influence constitutive modeling approaches in rock mechanics. Table 2 summarizes the analytical models reviewed based on their key assumptions, governing formulas, and major limitations. To facilitate practical model selection, a guideline framework linking rock-mass characteristics, available discontinuity information, and suitable analytical approaches is proposed in Table 3.

Table 2. Summary of analytical models for estimating the deformation modulus of jointed rock masses

Classification Basis	Researcher	Model characteristics/assumptions	Equation	Limitations and remarks
Equivalent-Continuum Compliance Models	Duncan and Goodman [51]	First finite-element compliance model for jointed rocks; discontinuities treated as zero-thickness elements with linear normal and shear stiffnesses; foundation for equivalent-continuum formulation.	$\frac{1}{E_m}=\frac{1}{E_r}+\frac{1}{k_nS}$ $\frac{1}{G_m}=\frac{1}{G_r}+\frac{1}{k_sS}$	Valid for small deformations and linear joint behavior; neglects joint–joint interaction; assumes uniform spacing and isotropic joint distribution.
	Singh [52]	General compliance-matrix formulation; incorporates joint stiffness, spacing, and orientation; explicit derivation of directional deformability using matrix representation.	$\frac{1}{E_m}=\frac{1}{E_r}+\frac{n}{k_n}$ $\frac{1}{G_m}=\frac{1}{G_r}+\frac{n}{k_s}$	Based on linear elasticity and independent joint sets; ignores joint intersection, stress concentration, and nonlinear closure effects.
	Singh [53]	Extension of the previous formulation to study anisotropy; demonstrated a greater reduction in shear modulus than in deformation modulus.	$(s_n/S_n)(k_n/k_s)\ \alpha\ G_m/E_m$	Suitable only for low stress gradients; overestimates lateral deformation in soft or densely jointed rocks.
	Kulhawy [54]	Three orthogonal, persistent joint sets; deformability expressed as a function of joint spacing and stiffness; introduced a semi-empirical correlation with RQD.	$\frac{1}{E_i}=\frac{1}{E_r}+\frac{1}{k_{i,n}S_i}$ $\frac{1}{G_{ij}}=\frac{1}{G_r}+\frac{1}{k_{j,s}S_j}$	Assumes orthogonal, regularly spaced, zero-thickness joints and linear elastic behavior; limited for irregular or intersecting joint systems; RQD correlation is empirical.
	Dershowitz et al. [55]	Probabilistic compliance formulation using joint-spacing–orientation probability function; stochastic averaging of deformation and shear moduli.	$\langle E_m\rangle=\int P(s,\theta)[E(s,\theta)]ds\,d\theta$ $\langle G_m\rangle=\int P(s,\theta)[G(s,\theta)]ds\,d\theta$	Valid for small strain and linear joint stiffness; assumes independent joint motion and homogeneous stress field; idealized boundary conditions.
Orthorhombic and 3D Equivalent Models	Salamon [56]	Transversely isotropic layered continuum with five independent elastic constants; deformability derived from strain-energy equivalence and harmonic averaging of layer moduli.	$E_1=(\sum\frac{\varphi_i}{E_{1i}})^{-1}, E_2=(\sum\frac{\varphi_i}{E_{2i}})^{-1}$, $G_2=(\sum\frac{\varphi_i}{G_{2i}})^{-1}$	Assumes perfect interlayer bonding and linear elasticity; neglects interlayer slip; valid for stratified formations rather than discrete jointed rocks.
	Amadei and Goodman [57]	First fully 3D equivalent-continuum model combining intact-rock and joint compliances; orthogonal, zero-thickness, linearly elastic joints; predicts direction-dependent stiffness and anisotropy.	$E_x=\left(\frac{1}{E_r}+\frac{1}{k_{nx}S_x}\right)^{-1}$ $G_{xy}=\left(\frac{1}{G_r}+\frac{1}{k_{sx}S_x}\right)^{-1}$	Linear-elastic assumption; ignores joint–joint interaction and slip; applicable to pre-yield, small-strain conditions.
	Gerrard [58]	Orthorhombic equivalent model for 1–3 orthogonal joint sets; emphasizes anisotropic stiffness reduction due to shear deformation; assumes thin, non-dilatant joints.	$E_y=\left(\frac{1}{E_r}+\frac{1}{k_{ny}S_y}\right)^{-1}$ $G_{yz}=\left(\frac{1}{G_r}+\frac{1}{k_{sy}S_y}\right)^{-1}$	Assumes linearly elastic, small-strain behavior; not valid for non-orthogonal or highly deformable joint geometries.
	Amadei and Savage [59]	Generalized orthorhombic equivalent-continuum model for non-orthogonal joint systems; includes directional dependence through orientation factor $f(\theta_i)$; links stiffness anisotropy with strength reduction.	$E_m(\theta)=\left[\sum_i\frac{1}{E_r}+\frac{f(\theta_i)}{k_{ni}S_i}\right]^{-1}$	Linear-joint assumption; small-strain, elastic range only; neglects joint-intersection interaction; suitable for regular joint networks under uniform loading.
Tensorial Crack and Fabric Models	Oda [60]	Introduced the second-order fabric tensor to statistically represent the orientation and density of discontinuities; a purely geometrical model describing directional bias in joint systems.	$F_{ij}=\int n_in_jE(n)d\Omega$	Geometrical only – no mechanical coupling; accuracy decreases for clustered or non-random joints.
	Oda [61]	Developed the first tensorial compliance formulation using a fourth-order crack tensor (F_{ijkl}) establishing mechanical linkage between crack geometry and elastic anisotropy.	$\varepsilon_{ij}=\alpha F_{ijkl}\sigma_{kl}+D^0_{ijkl}\sigma_{kl}$	Assumes linear elasticity and low crack density; neglects crack interactions and stress-dependent closure.

Classification Basis	Researcher	Model characteristics/assumptions	Equation	Limitations and remarks
	Oda [62]	Hydro-mechanically coupled extension of the tensorial framework; relates stress–strain behavior to fracture-controlled permeability through joint stiffness and spacing.	$\varepsilon_{ij} = M_{ijkl}\sigma_{kl} + (p\delta_{kl} - C_{ijkl}\sigma_{kl})$	Requires laboratory calibration of joint stiffness and pressure data; valid mainly in the elastic regime; neglects nonlinear joint closure.
	Oda [63]	Experimental validation on mylonite specimens; proposed empirical stiffness-reduction laws derived from fabric-tensor components linking crack density to modulus degradation.	$\frac{E'}{E} = \frac{1}{1+\alpha F_{11}} \quad \frac{G'}{G} = \frac{1}{1+\beta F_{ij}}$	Applicable to small-strain, elastic behavior; assumes random, non-interacting cracks and isotropic matrix.
Isotropization by Random Averaging Models	Fossum [64]	Closed-form isotropic model derived from composite-material averaging; joints assumed to be randomly oriented and uniformly distributed; deformation governed by joint spacing S and joint stiffnesses k_n, k_s;provides analytical expressions for effective bulk and shear moduli.	$E_m = \frac{9K_mG_m}{3K_m+G_m}$ $G_m = \frac{1}{30}\left[\frac{E_r}{(1+\upsilon_r)}\frac{9(1+\upsilon_r)(1-2\upsilon_r)sk_n + (7-5\upsilon_r)E_r}{(1+\upsilon_r)(1-2\upsilon_r)sk_n + (1-\upsilon_r)E_r}\right] + \frac{2}{5}\left[\frac{E_r sk_s}{2(1+\upsilon_r)sk_s + E_r}\right]$	Assumes linear elasticity, random and isotropic joint distribution, and small strains; neglects joint interaction and nonlinearity; not valid for directional or high-density jointing.
Joint-Stiffness–Driven Laboratory Models	Yoshinaka and Yamabe [65]	Laboratory-calibrated analytical model directly linking joint normal and shear stiffnesses—measured from laboratory tests—to the equivalent deformation and shear moduli of jointed rock masses; assumes linearly elastic, zero-thickness joints and independent orthogonal joint sets.	$E_t = \left[\frac{1}{E_r} + \frac{\cos^2\theta_1}{L_1}\left(\frac{\sin^2\theta_1}{k_{s1}} + \frac{\cos^2\theta_1}{k_{n1}}\right) + \frac{\cos^2\theta_2}{L_2}\left(\frac{\sin^2\theta_2}{k_{s2}} + \frac{\cos^2\theta_2}{k_{n2}}\right)\right]^{-1}$ $G_t = \left[\frac{2(1+\upsilon_r)}{E_r} + \frac{\cos^2\theta_1}{L_1}\left(\frac{2\sin^2\theta_1 + \lvert\sin\theta_1\rvert 2}{k_{s1}} + \frac{2\cos^2\theta_1 - \lvert\sin}{k_{n1}}\right.\right.$ $\left.\left.\frac{\cos^2\theta_2}{L_2}\left(\frac{2\sin^2\theta_2 + \lvert\sin 2\theta_2\rvert 2}{k_{s2}} + \frac{2\cos^2\theta_2 - \lvert\sin 2\theta_2\rvert}{k_{n2}}\right.\right.\right.$	Excludes dilatancy and shear–normal coupling; valid for small-strain, pre-yield conditions and orthogonal joint sets; nonlinear effects under high confining pressures not represented.
Non-Orthogonal and Dilatancy-Inclusive Models	Chen [66]	Nonlinear ubiquitous-joint constitutive model for orthogonal joint sets; captures joint closure, slip, and post-peak softening; assumes plane-strain, linear-elastic matrix, and nonlinear joint stiffness.	$\varepsilon_{ij} = \sum_k \varepsilon_{ij}^m + \varepsilon_{ij}^{(k)}$	Joint sets; no explicit modulus expressions; requires numerical calibration for post-peak behavior.
	Huang et al. [67]	Analytical 3-D non-orthogonal model; incorporates intersection angle θ, joint spacing, and normal/shear stiffness (k_n, k_s); accounts for dilatancy through coupling between shear displacement and volumetric strain.	$\frac{1}{E_y} = 2\sin^2(\frac{\theta}{2})\frac{\cos^2(\frac{\theta}{2})k_n + \sin^2(\frac{\theta}{2})k_s}{k_n k_s s}$ $\frac{1}{G_{xy}} = \frac{1}{k_{s3}s_3} + \frac{2\sin\theta\cos^2(\frac{\theta}{2})}{k_s s}$	Complex calibration; assumes small-strain linearity and uniform stress; provides lower-bound modulus due to neglect of joint interaction and stress heterogeneity.
Advanced Hybrid and Nonlinear Models	Kulatilake et al. [68]	Hybrid analytical–numerical framework combining fracture-tensor statistics with 3DEC simulations; considers finite joint size, density, and persistence; semi-analytical power-law relations derived from numerical data.	$B(F_{ij})^\beta = A_{ij}(F_{ii})^\alpha \quad G = E_i$	Invalid for infinite joint persistence; DEM calibration required; scale-sensitive and semi-empirical.
	Wang and Huang [69]	Nonlinear multi-joint constitutive model; includes pre- and post-peak deformation, joint closure, slip, and dilatancy; implemented in FLAC.	$d\varepsilon = \sum_a d\varepsilon_a^J + d\varepsilon^I$	No closed-form modulus; requires iterative tangent-modulus computation; parameter- and calibration-sensitive.
	Zhang [70]	Simplified isotropic averaging formulation for heavily jointed rocks; practical closed-form extension of Fossum's model including spacing and stiffness contrast.	$E_m = \frac{1}{\frac{1}{E_r} + \frac{1}{3}\left[\frac{21}{32k_n s} + \frac{11}{32k_s s}\right]}$ $G_m = \frac{1}{\frac{1}{G_r} + \frac{1}{3}\left[\frac{11}{32k_n s} + \frac{21}{32k_s s}\right]}$	Assumes random jointing; limited for strong structural anisotropy; reduced accuracy for ordered joint systems.

Table 3. Practical framework for selecting deformation-modulus models based on rock-mass characteristics and available discontinuity information

Rock condition	Available information	Recommended approach
Moderately jointed rock masses with relatively regular discontinuities	Joint spacing, stiffness, and frequency	Equivalent-Continuum Compliance Models
Strongly anisotropic rock masses with dominant joint sets	Joint orientation and directional stiffness	Orthorhombic and 3D Equivalent Models
Randomly fractured rock masses with statistically distributed discontinuities	Statistical fracture orientation, density, and fabric characteristics	Tensorial Crack and Fabric Models
Rock masses with approximately isotropic discontinuity distributions	Statistical distribution of joint orientations and average joint properties	Random-isotropic averaging model
Rock masses with experimentally or field-characterized joint mechanical properties	Normal and shear joint stiffness, joint surface properties, and stress conditions	Joint stiffness driven laboratory model
Rock masses affected by non-orthogonal joints, closure, dilatancy, or nonlinear response	Joint orientation, intersection geometry, stress dependency, and dilatancy behavior	Nonorthogonal and dilatancy-inclusive Models
Highly fractured rock masses with complex fracture geometry, scale effects, or stress-dependent deformation	Finite fracture size, persistence, fracture interaction, nonlinear joint behavior, and calibration data	Advanced Hybrid and Nonlinear Models

4. Discussion

The synthesis of twenty analytical formulations developed between 1968 and 2010 reveals a clear and progressive evolution in the theoretical understanding of the rock mass deformation modulus. The early compliance-based group of models provided the first physically grounded attempts to express rock mass deformability as the additive contribution of intact rock and joint components. This first generation of formulations established the linear elastic foundation for subsequent analytical developments. Despite their simplicity, these models introduced essential mechanical parameters such as joint stiffness, spacing, and frequency, which remain fundamental to later analytical, numerical, and data-driven frameworks.

The transition from scalar compliance relations to tensorial and orthorhombic model groups during the 1980s represented a major conceptual advance in analytical rock mechanics. This generation of models introduced tensor-based formulations capable of explicitly representing anisotropy and direction-dependent stiffness. Through the adoption of fabric and crack-tensor concepts, these frameworks systematically linked the statistical geometry of discontinuities with the macroscopic mechanical response, culminating in experimental validation of tensorial theories toward the late 1980s. Collectively, this group of studies demonstrated that deformation modulus reduction correlates with increasing crack density and orientation bias, while shear compliance exerts the dominant control on the overall deformability of jointed rock masses. Although these formulations were limited to small-strain and linear-elastic conditions, their tensorial structure provided the theoretical groundwork for later nonlinear and hybrid approaches.

The next generation, represented by the random-isotropic averaging group, extended analytical formulations by statistically integrating joint orientations through composite-material theory, yielding closed-form expressions for randomly jointed rocks without experimental calibration. In parallel, the laboratory-based joint stiffness group advanced analytical modeling by directly linking experimentally measured joint stiffnesses to the equivalent deformation and shear moduli of jointed rock masses. These laboratory-calibrated formulations demonstrated that mean joint spacing and stiffness jointly govern the scale-dependent reduction of the modulus and provided a practical framework for field implementation. Nevertheless, both model groups relied on linear stiffness assumptions and idealized geometries, which limited their accuracy for highly anisotropic or densely fractured systems.

The emergence of nonlinear and dilatancy-inclusive frameworks marked a turning point in analytical model development. These models incorporated pre- and post-peak joint behavior, shear slip, and volumetric expansion. Although they introduced additional complexity and required calibration, their inclusion of nonlinear joint closure and dilatancy mechanisms significantly improved the physical realism of analytical predictions.

The hybrid and semi-analytical model group of the 1990s and 2000s marked the convergence of analytical and numerical methodologies. These models bridged the gap between theoretical rigor and practical applicability, forming the foundation for hybrid constitutive modeling in modern

computational rock mechanics. Methodologically, this generation represented three parallel advances: analytical formulations became progressively tensorial and nonlinear, mechanical realism expanded to include stress-dependent and dilatancy-coupled behavior, and computational integration evolved toward semi-analytical frameworks suited for numerical implementation. Despite such progress, limitations remain. Most models still assume simplified joint geometries, continuous and non-interacting discontinuities, and small-strain behavior, which restrict their applicability to natural rock masses. Moreover, only a few account for stress-path dependence, time effects, or progressive damage. While hybrid formulations alleviate some of these issues, they often depend on numerical or experimental calibration, limiting their complete analytical generality.

Compared with empirical approaches commonly used for estimating the rock-mass deformation modulus, equivalent-continuum compliance models provide a mechanically based representation by explicitly incorporating discontinuity characteristics, including joint stiffness, spacing, frequency, and orientation. Empirical methods, such as those based on rock-mass classification systems, remain valuable for preliminary design and engineering applications where detailed discontinuity information is unavailable due to their simplicity and limited data requirements. However, their predictive capability is generally dependent on the empirical database and geological conditions from which they were developed. In contrast, equivalent-continuum models can provide a more physically meaningful interpretation of deformation mechanisms when representative discontinuity parameters are available. Nevertheless, these models do not universally provide higher accuracy, because their reliability depends strongly on the quality of input parameters and the validity of homogenization assumptions. Therefore, model selection should be governed by rock-mass characteristics, available discontinuity information, and the dominant deformation mechanism. As summarized in Table 3, simplified compliance-based models are more suitable for moderately jointed rock masses, whereas tensorial, nonlinear, and hybrid analytical–numerical approaches become more appropriate for cases involving anisotropy, complex fracture networks, scale effects, or stress-dependent deformation behavior.

Future research should therefore aim to combine analytical transparency with data-driven adaptability. Developing hybrid or physics-informed machine learning models could preserve the mechanistic clarity of analytical formulations while enhancing predictive flexibility. Embedding analytical constitutive relations as constraints within numerical or ML-based frameworks would enable physically consistent yet adaptive deformability predictions across different scales and geological conditions.

5. Conclusions

This review evaluated twenty analytical and semi-analytical models proposed between 1968 and 2010 for estimating the deformation modulus of jointed rock masses. The collective evidence shows a consistent evolution from simple linear compliance relations toward hybrid, nonlinear, and physically enriched constitutive formulations. Early compliance and orthorhombic theories established the mathematical basis for representing anisotropy, whereas later tensorial and isotropic averaging models incorporated joint geometry and stiffness more explicitly into deformation analysis.

The findings indicate that joint stiffness, spacing, and orientation remain the dominant parameters governing rock mass deformability across all analytical generations. Among them, shear compliance exerts a stronger influence than normal compliance, explaining the pronounced reduction of shear modulus under jointed conditions. Although significant advances have been made, most analytical models are still constrained by simplified geometries, linear elastic assumptions, and the omission of stress-path or scale effects.

Future progress in analytical modeling should focus on bridging mechanistic frameworks with data-driven and numerical approaches. Integrating analytical principles with modern computational methods, such as physics-informed neural networks or hybrid constitutive solvers, offers a promising avenue for developing predictive yet interpretable formulations applicable across scales and geological conditions. Such integration can preserve the transparency of analytical models while enhancing their adaptability and predictive power. Overall, the analytical developments synthesized in this review provide a robust theoretical foundation for understanding rock-mass deformability.

References

[1]. Palmström, A., & Singh, R. (2001). The deformation modulus of rock masses—comparisons between in situ

tests and indirect estimates. *Tunnelling and Underground Space Technology*, *16*(2), 115–131.

[2]. Barton, N. (2002). Some new Q-value correlations to assist in site characterisation and tunnel design. *International Journal of Rock Mechanics and Mining Sciences, 39*(2), 185–216.

[3]. Dodds, D. J. (1974). Interpretation of plate loading test results. ASTM International, West Conshohocken, PA.

[4]. Misterek, D. L., Slebir, E. J., & Montgomery, J. S. (1974). Conducting uniaxial jacking tests. *Field Testing and Instrumentation of Rock*, ASTM Special Technical Publication, *554*, 35.

[5]. Alexander, L. G. (1960). Field and laboratory tests in rock mechanics. In *Proceedings of the Third Australian-New Zealand Conference on Soil Mechanics and Foundation Engineering* (pp. 161–168).

[6]. Deklotz, E. J., & Boisen, B. P. (1970). Development of equipment for determining deformation modulus and in situ stress by means of large flatjacks. *ASTM Special Technical Publication*, *477*, 117–125.

[7]. Vogler, U. W., Deere, D. U., & Bieniawski, Z. T. (1976). CSIR large flat jack equipment for determining rock mass deformability.

[8]. Pratt, H. R., & Black, A. D. (1974). A new technique for determining the deformation modulus of rock masses. *Field Testing and Instrumentation of Rock,* ASTM Special Technical Publication, *554*, 3.

[9]. Van Heerden, W. L. (1976). In-situ rock mass property test. Geomechanics Division, National Mechanical Engineering Research Institute, Council for Scientific and Industrial Research.

[10]. Bowcock, J. B., Merritt, J. M., Hoek, E., & Singh, J. C. (1976). Drakensberg pumped storage scheme: rock engineering aspects.

[11]. Misterek, D. L. (1970). Analysis of data from radial jacking tests. ASTM International, pp. 27–38.

[12]. Bieniawski, Z. T., & Van Heerden, W. L. (1975). The significance of in situ tests on large rock specimens. *International Journal of Rock Mechanics and Mining Sciences & Geomechanics Abstracts*, *12*(4), 101–113.

[13]. Rocha, M. (1974). Present possibilities of studying foundations of concrete dams. In *Proceedings of the 3rd International Congress on Rock Mechanics* (Vol. IA, pp. 879–896). International Society for Rock Mechanics, Denver.

[14]. Goodman, R. E., Van, T. K., & Heuze, F. E. (1968). Measurement of rock deformability in boreholes. In *Proceedings of ARMA US Rock Mechanics/Geomechanics Symposium*. ARMA.

[15]. Heuze, F. E., & Salem, A. (1977). Rock deformability measured in situ—problems and solutions. In *Proceedings of International Congress on Field Measurements in Rock Mechanics (FMRM 77)* (pp. 375–387).

[16]. Bieniawski, Z. T. (1978). Determining rock mass deformability: experience from case histories. *International Journal of Rock Mechanics and Mining Sciences & Geomechanics Abstracts*, *15*(5), 237–247.

[17]. Deere, D. U., Hendron, A. J., Patton, F. D., & Cording, E. J. (1966). Design of surface and near-surface construction in rock. In *Proceedings of ARMA US Rock Mechanics/Geomechanics Symposium*. ARMA.

[18]. Coon, R. F., & Merritt, A. H. (1970). Predicting in situ modulus of deformation using rock quality indexes. ASTM International, West Conshohocken, PA.

[19]. Gardner, W. S. (1987). Design of drilled piers in the Atlantic Piedmont. In *Foundations and Excavations in Decomposed Rock of the Piedmont Province* (pp. 62–86). ASCE.

[20]. Kayabasi, A., Gokceoglu, C., & Ercanoglu, M. (2003). Estimating the deformation modulus of rock masses: a comparative study. *International Journal of Rock Mechanics and Mining Sciences*, *40*(1), 55–63.

[21]. Gokceoglu, C., Sonmez, H., & Kayabasi, A. (2003). Predicting the deformation moduli of rock masses. *International Journal of Rock Mechanics and Mining Sciences*, *40*(5), 701–710.

[22]. Zhang, L., & Einstein, H. H. (2004). Using RQD to estimate the deformation modulus of rock masses. *International Journal of Rock Mechanics and Mining Sciences*, *41*(2), 337–341.

[23]. Serafim, J. L., & Pereira, J. P. (1983). Considerations of the geomechanics classification of Bieniawski. In *Proceedings International Symposium Engineering Geology and Underground Construction* (Vol. 1, pp. II33–II42). Lisbon.

[24]. Nicholson, G. A., & Bieniawski, Z. T. (1990). A nonlinear deformation modulus based on rock mass classification. *International Journal of Mining and Geological Engineering*, *8*(3), 181–202.

[25]. Mehrotra, V. K. (1992). Estimation of engineering parameters of rock mass. University of Roorkee.

[26]. Mitri, H. S., Edrissi, R., & Henning, J. G. (1995). Finite-element modeling of cable-bolted stopes in hard-rock underground mines. *Transactions-Society for Mining, Metallurgy and Exploration Incorporated*, *298*, 1897–1902.

[27]. Aydan, Ö., Ulusay, R., & Kawamoto, T. (1997). Assessment of rock mass strength for underground excavations. *International Journal of Rock Mechanics and Mining Sciences*, *34*(3–4), 18e1.

[28]. Read, S. A. L., Perrin, N. D., & Richards, L. R. (1999). Applicability of the Hoek-Brown failure criterion to New Zealand greywacke rocks. In *ISRM Congress*. ISRM.

[29]. Diederichs, M. S., & Kaiser, P. K. (1999). Stability of large excavations in laminated hard rock masses: the voussoir analogue revisited. *International Journal of Rock Mechanics and Mining Sciences*, *36*(1), 97–117.

[30]. Ramamurthy, T. (2004). A geo-engineering classification for rocks and rock masses. *International Journal of Rock Mechanics and Mining Sciences, 41*(1), 89–101.

[31]. Sonmez, H., Gokceoglu, C., Nefeslioglu, H. A., & Kayabasi, A. (2006). Estimation of rock modulus: for intact rocks with an artificial neural network and for rock masses with a new empirical equation. *International Journal of Rock Mechanics and Mining Sciences, 43*(2), 224–235.

[32]. Chun, B. S., Lee, Y. J., Seo, D. D., & Lim, B. S. (2006). Correlation deformation modulus by PMT with RMR and rock mass condition. *Tunnelling and Underground Space Technology incorporating Trenchless Technology Research*, *21*(3), 231–232.

[33]. Galera, J. M., Álvarez, M., & Bieniawski, Z. T. (2007). Evaluation of the deformation modulus of rock masses using RMR. Comparison with dilatometer tests. In *Workshop: Underground Works under Special Conditions*.

[34]. Isik, N. S., Ulusay, R., & Doyuran, V. (2008). Deformation modulus of heavily jointed–sheared and blocky greywackes by pressuremeter tests: numerical, experimental and empirical assessments. *Engineering Geology*, *101*(3–4), 269–282.

[35]. Mohammadi, H., & Rahmannejad, R. (2010). The estimation of rock mass deformation modulus using regression and artificial neural networks analysis. *Arabian Journal for Science and Engineering*, *35* (1), 205.

[36]. Shen, J., Karakus, M., & Xu, C. (2012). A comparative study for empirical equations in estimating deformation modulus of rock masses. *Tunnelling and Underground Space Technology*, *32*, 245–250.

[37]. Kang, S. S., Kim, H. Y., & Jang, B. A. (2013). Correlation of in situ modulus of deformation with degree of weathering, RMR and Q-system. *Environmental Earth Sciences*, *69* (8), 2671–2678.

[38]. Khabbazi, A., Ghafoori, M., Lashkaripour, G. R., & Cheshomi, A. (2013). Estimation of the rock mass deformation modulus using a rock classification system. *Geomechanics and Geoengineering*, *8* (1), 46–52.

[39]. Kavur, B., Cvitanović, N. Š., & Hrženjak, P. (2015). Comparison between plate jacking and large flat jack test results of rock mass deformation modulus. *International Journal of Rock Mechanics and Mining Sciences*, *73*, 102–114.

[40]. Alemdag, S., Gurocak, Z., & Gokceoglu, C. (2015). A simple regression-based approach to estimate deformation modulus of rock masses. *Journal of African Earth Sciences*, *110*, 75–80.

[41]. Barton, N., Løset, F., Lien, R., & Lunde, J. (1980). Application of the Q-system in design decisions. In *Sub Surface Space,* Vol. 2.

[42]. Barton, N. (1996). Estimating rock mass deformation modulus for excavation disturbed zone studies. In *International Conference on Deep Geological Disposal of Radioactive Waste, EDZ Workshop* (pp. 133–144). Canadian Nuclear Society.

[43]. Ajalloeian, R., & Mohammadi, M. (2014). Estimation of limestone rock mass deformation modulus using empirical equations. *Bulletin of Engineering Geology and the Environment*, *73* (2), 541–550.

[44]. Hoek, E., & Brown, E. T. (1997). Practical estimates of rock mass strength. *International Journal of Rock Mechanics and Mining Sciences*, *34* (8), 1165–1186.

[45]. Hoek, E., Carranza-Torres, C., & Corkum, B. (2002). Hoek-Brown failure criterion—2002 edition. In *Proceedings of NARMS-Tac* (Vol. 1, pp. 267–273).

[46]. Sonmez, H., Gokceoglu, C., & Ulusay, R. (2004). Indirect determination of the modulus of deformation of rock masses based on the GSI system. *International Journal of Rock Mechanics and Mining Sciences*, *41* (5), 849–857.

[47]. Hoek, E., & Diederichs, M. S. (2006). Empirical estimation of rock mass modulus. **International Journal of Rock Mechanics and Mining Sciences, 43* (2), 203–215.

[48]. Sanei, M., Rahmati, A., Faramarzi, L., Goli, S., & Mehinrad, A. (2013). Estimation of rock mass deformation modulus in Bakhtiary Dam Project in Iran. In *ISRM SINOROCK*. ISRM.

[49]. Palmström, A. (1995). RMi—a rock mass characterization system for rock engineering purposes.

[50]. Rowe, R. K., & Armitage, H. H. (1984). The design of piles socketed into weak rock. Faculty of Engineering Science, University of Western Ontario.

[51]. Duncan, J. M., & Goodman, R. E. (1968). Finite element analyses of slopes in jointed rock. Technical Report TE681.

[52]. Singh, B. (1973). Continuum characterization of jointed rock masses: Part I—The constitutive equations. *International Journal of Rock Mechanics and Mining Sciences & Geomechanics Abstracts*, *10* (4), 311–335.

[53]. Singh, B. (1973). Continuum characterization of jointed rock masses: Part II—Significance of low shear modulus. *International Journal of Rock Mechanics and Mining Sciences & Geomechanics Abstracts*, *10* (4), 337–349.

[54]. Kulhawy, F. H. (1978). Geomechanical model for rock foundation settlement. *Journal of the Geotechnical Engineering Division*, *104* (2), 211–227.

[55]. Dershowitz, W., Baecher, G., & Einstein, H. (1979). Prediction of rock mass deformability. In *ISRM Congress*.

[56]. Salamon, M. D. G. (1968). Elastic moduli of a stratified rock mass. *International Journal of Rock Mechanics and Mining Sciences & Geomechanics Abstracts, 5* (6), 519–527.

[57]. Amadei, B., & Goodman, R. E. (1981). A 3-D constitutive relation for fractured rock masses. In *Proceedings of the International Symposium on the Mechanical Behavior of Structured Media* (pp. 249–268).

[58]. Gerrard, C. M. (1982). Elastic models of rock masses having one, two and three sets of joints. *International Journal of Rock Mechanics and Mining Sciences & Geomechanics Abstracts*, *19* (1), 15–23.

[59]. Amadei, B., & Savage, W. Z. (1993). Effect of joints on rock mass strength and deformability. In *Comprehensive Rock Engineering* (Vol. 1, pp. 331–365).

[60]. Oda, M. (1982). Fabric tensor for discontinuous geological materials. *Soils and Foundations*, *22* (4), 96–108.

[61]. Oda, M., Suzuki, K., & Maeshibu, T. (1984). Elastic compliance for rock-like materials with random cracks. *Soils and Foundations*, *24*(3), 27–40.

[62]. Oda, M. (1986). An equivalent continuum model for coupled stress and fluid flow analysis in jointed rock masses. *Water Resources Research*, *22*(13), 1845–1856.

[63]. Oda, M. (1988). An experimental study of the elasticity of mylonite rock with random cracks. *International Journal of Rock Mechanics and Mining Sciences & Geomechanics Abstracts, 25*(2), 59–69.

[64]. Fossum, A. F. (1985). Effective elastic properties for a randomly jointed rock mass. *International Journal of Rock Mechanics and Mining Sciences & Geomechanics Abstracts, 22*(6), 467–470.

[65]. Yoshinaka, R., & Yamabe, T. (1986). Joint stiffness and the deformation behaviour of discontinuous rock. *International Journal of Rock Mechanics and Mining Sciences & Geomechanics Abstracts*, *23*(1), 19–28.

[66]. Chen, E. P. (1989). A constitutive model for jointed rock mass with orthogonal sets of joints.

[67]. Huang, T. H., Chang, C. S., & Yang, Z. Y. (1995). Elastic moduli for fractured rock mass. *Rock Mechanics and Rock Engineering, 28*(3), 135–144.

[68]. Kulatilake, P. H., Wang, S., & Stephansson, O. (1993). Effect of finite size joints on the deformability of jointed rock in three dimensions. *International Journal of Rock Mechanics and Mining Sciences & Geomechanics Abstracts*, *30*(5), 479–501.

[69]. Wang, T. T., & Huang, T. H. (2009). A constitutive model for the deformation of a rock mass containing sets of ubiquitous joints. *International Journal of Rock Mechanics and Mining Sciences*, *46*(3), 521–530.

[70]. Zhang, L. (2010). Method for estimating the deformability of heavily jointed rock masses. *Journal of Geotechnical and Geoenvironmental Engineering, 136*(9), 1242–1250.

[71]. Wu, Q., & Kulatilake, P. H. S. W. (2012). REV and its properties on fracture system and mechanical properties, and an orthotropic constitutive model for a jointed rock mass in a dam site in China. *Computers and Geotechnics*, *43*, 124–142.

[72]. Bidgoli, M. N., Zhao, Z., & Jing, L. (2013). Numerical evaluation of strength and deformability of fractured rocks. *Journal of Rock Mechanics and Geotechnical Engineering*, *5*(6), 419–430.

[73]. Khani, A., Baghbanan, A., & Hashemolhosseini, H. (2013). Numerical investigation of the effect of fracture intensity on deformability and REV of fractured rock masses. *International Journal of Rock Mechanics and Mining Sciences*, *63*, 104–112.

[74]. Alshkane, Y. M., Marshall, A. M., & Stace, L. R. (2017). Prediction of strength and deformability of an interlocked blocky rock mass using UDEC. *Journal of Rock Mechanics and Geotechnical Engineering*, *9*(3), 531–542.

[75]. Laghaei, M., Baghbanan, A., Hashemolhosseini, H., & Dehghanipoodeh, M. (2018). Numerical determination of deformability and strength of 3D fractured rock mass. *International Journal of Rock Mechanics and Mining Sciences*, *110*, 246–256.

[76]. Jaberi, A., & Zare, S. (2026). Numerical evaluation of the influence of fracture geometry parameter on deformability, strength, and Poisson's ratio of 3D-fractured rock. *Indian Geotechnical Journal*, *56*(2), 772-791.

[77]. Jaberi, A., & Zare, S. (2025). The effect of non-persistent and persistent joint angles on the representative elementary volume rock mass based on strength. *Journal of Mining and Environment*, *16*(3), 1141–1151.

[78]. Beiki, M., Bashari, A., & Majdi, A. (2010). Genetic programming approach for estimating the deformation modulus of rock mass using sensitivity analysis by neural network. *International Journal of Rock Mechanics and Mining Sciences*, *47*(7), 1091–1103.

[79]. Asadizadeh, M., & Hossaini, M. F. (2016). Predicting rock mass deformation modulus by artificial intelligence approach based on dilatometer tests. *Arabian Journal of Geosciences, 9* (2), 96.

[80]. Ghasemi, E., Kalhori, H., Bagherpour, R., & Yagiz, S. (2018). Model tree approach for predicting uniaxial compressive strength and Young's modulus of carbonate rocks. *Bulletin of Engineering Geology and the Environment*, *77*(1), 331–343.

[81]. Ceryan, N., Ozkat, E. C., Korkmaz Can, N., & Ceryan, S. (2021). Machine learning models to estimate the elastic modulus of weathered magmatic rocks. *Environmental Earth Sciences*, *80*(12), 448.

[82]. Cao, J., Gao, J., Nikafshan Rad, H., Mohammed, A. S., Hasanipanah, M., & Zhou, J. (2022). A novel systematic and evolved approach based on XGBoost-firefly algorithm to predict Young's modulus and unconfined compressive strength of rock. *Engineering with Computers*, *38*(Suppl 5), 3829–3845.

[83]. Tokgozoglu, K., Aladag, C. H., & Gokceoglu, C. (2023). Artificial neural networks to predict deformation modulus of rock masses considering overburden stress. Geomechanics and Geoengineering, *18*(1), 48–64.

[84]. Shahverdiloo, M. R., & Zare, S. (2026). A genetic programming model for estimating the rock mass deformation modulus based on analytical parameters and in situ stress. *Tunnelling and Underground Space Technology*, *168*, 107073.

[85]. Zhang, L. (2016). *Engineering properties of rocks*. Butterworth-Heinemann.

[86]. Ramamurthy, T. (2001). Shear strength response of some geological materials in triaxial compression. *International Journal of Rock Mechanics and Mining Sciences*, *38*(5), 683–697.

[87]. Chun, B. S., Ryu, W. R., Sagong, M., & Do, J. N. (2009). Indirect estimation of the rock deformation modulus based on polynomial and multiple regression analyses of the RMR system. *International Journal of Rock Mechanics and Mining Sciences*, *46*(3), 649–658.

[88]. Martins, F. F., & Miranda, T. F. (2012). Estimation of the rock deformation modulus and RMR based on data mining techniques. *Geotechnical and Geological Engineering*, *30*(4), 787–801.

[89]. Nejati, H. R., Ghazvinian, A., Moosavi, S. A., & Sarfarazi, V. (2014). On the use of the RMR system for estimation of rock mass deformation modulus. *Bulletin of Engineering Geology and the Environment*, *73* (2), 531–540.

[90]. Kallu, R. R., Keffeler, E. R., Watters, R. J., & Agharazi, A. (2015). Development of a multivariate empirical model for predicting weak rock mass modulus. *International Journal of Mining Science and Technology*, *25*(4), 545–552.

نشریه مهندسی معدن و محیط زیست
نشانی نشریه: www.jme.shahroodut.ac.ir
انجمن مهندسی معدن ایران
دانشگاه صنعتی شاهرود

مروری انتقادی بر رویکردهای تحلیلی و نیمه‌تحلیلی برای برآورد مدول تغییرشکل توده‌سنگ‌های درزه‌دار

عارف جابری*، و شکراله زارع

دانشکده مهندسی معدن، نفت و ژئوفیزیک، دانشگاه صنعتی شاهرود، شاهرود، ایران

اطلاعات مقاله

تاریخ ارسال: ۲۰۲۶/۰۸/۱۴
تاریخ داوری: ۲۰۲۶/۰۹/۰۵
تاریخ پذیرش: ۲۰۲۶/۰۹/۲۸

DOI: 10.22044/jme.2026.18187.3624

کلمات کلیدی

مدل‌های تحلیلی
مدل‌های نیمه تحلیلی
مدول تغییر شکل
توده سنگ درزه دار
مدل‌های محیط پیوسته معادل

چکیده

مدول تغییرشکل توده‌سنگ‌های درزه‌دار نقش مهمی در تعیین پایداری و تغییرشکل سازه‌های مهندسی سنگ ایفا می‌کند. با توجه به اهمیت مهندسی این پارامتر و پیچیدگی تغییرشکل کنترل‌شده توسط ناپیوستگی‌ها، رویکردهای متعددی با سطوح متفاوتی از دقت فیزیکی و محاسباتی برای برآورد آن توسعه یافته‌اند. در این مقاله مروری، بیست مدل تحلیلی و نیمه‌تحلیلی ارائه‌شده در فاصله سال‌های ۱۹۶۸ تا ۲۰۱۰ به‌صورت انتقادی بررسی شده‌اند. این مدل‌ها بر اساس ساختار ریاضی و فرضیات مکانیکی خود در هفت گروه شامل مدل‌های مبتنی بر کامپلاینس، مدل‌های ارتورومبیک و معادل سه‌بعدی، مدل‌های تانسوری ترک یا فابریک، مدل‌های میانگین‌گیری همسانگرد تصادفی، مدل‌های مبتنی بر سختی کالیبره‌شده آزمایشگاهی، مدل‌های غیرمتعامد و شامل اتساع، و فرمول‌بندی‌های ترکیبی غیرخطی طبقه‌بندی شده‌اند. نتایج نشان می‌دهند که سختی، فاصله‌داری و جهت‌گیری درزه‌ها مهم‌ترین عوامل کنترل‌کننده رفتار تغییرشکلی توده‌سنگ‌های درزه‌دار هستند و در این میان، نرمی برشی تأثیر غالبی دارد. با این حال، بیشتر مدل‌های تحلیلی همچنان بر هندسه‌های ساده‌شده، فرض رفتار الاستیک خطی و کرنش‌های کوچک استوار هستند که می‌تواند کاربرد آن‌ها را در توده‌سنگ‌های بسیار ناهمگن محدود سازد. پژوهش‌های آینده باید بر تلفیق شفافیت مدل‌های تحلیلی با قابلیت انطباق روش‌های داده‌محور تمرکز کنند؛ به‌ویژه استفاده از چارچوب‌های یادگیری ماشین آگاه از فیزیک که قادر به ترکیب درک سازوکارهای فیزیکی با انعطاف‌پذیری پیش‌بینی باشند.

نویسنده مسئول مکاتبات: Jaberi@shahroodut.ac.ir (ع. جابری)